EXAFS and IR Study of the CO-Adsorption-Induced Morphology Change in Ru Catalysts

Takanori Mizushima,† Kazuyuki Tohji,† Yasuo Udagawa,*,† and Akifumi Ueno‡

Contribution from the Institute for Molecular Science, Okazaki, Aichi 444, Japan, and Toyohashi University of Technology, Toyohashi, Aichi 440, Japan. *Received March 5, 1990*

Abstract: EXAFS (extended X-ray absorption fine structure) and IR studies were performed on Ru catalysts supported on γ-Al_2O_3, MgO, SiO_2, and TiO_2 to elucidate the mechanism of the CO adsorption-induced disruption of metal clusters. EXAFS results show that after reduction, Ru atoms exist on all supports as small metal clusters, but the particle sizes and metal–support interactions vary with the support. CO adsorption onto Ru/γ-Al_2O_3 and Ru/MgO led to the disruption of Ru–Ru bonds. By comparing with IR spectroscopic observations it is concluded that new species like O–Ru–CO and O–Ru–$(CO)_2$ on γ-Al_2O_3 and O_n–Ru–CO and $(O_n$–$Ru)_2$–CO (n = 3, 4) on MgO are formed after CO admission. On the other hand, no evidence of disruption of Ru clusters by CO adsorption was obtained in Ru/SiO_2 and Ru/TiO_2. The IR study showed, contrary to previously proposed models, that no H_2 evolution takes place during the CO adsorption-induced disruption. A new reaction scheme that is consistent with our observations is presented.

Introduction

A number of studies of CO molecules adsorbed on supported metal catalysts have been reported. The manner of CO adsorption can be studied with IR spectroscopy through the numbers and frequencies of C–O stretching vibrational modes. Sometimes the properties of supported metal atoms such as oxidation state and dispersion are also estimated through changes in absorption bands of the adsorbate molecules. For example, Rice et al.[1-3] characterized Rh atoms supported on several materials by the use of CO as a probe adsorbate. They concluded that Rh atoms supported on TiO_2 and SiO_2 are easily reduced to rhodium metal, while Al_2O_3-supported Rh catalysts consist of mostly nonmetallic rhodium, dispersed atomically and oxidized to 1+. Although IR study of adsorbed CO is a convenient and widely applied method to characterize supported catalysts, information obtained about the structure of metal aggregates is rather indirect.

EXAFS spectroscopy can directly determine local structures around metal atoms in dispersed catalysts. Using EXAFS, van't Blik et al. reported in a series of papers[4-6] straightforward evidence of a structural change in Rh clusters supported on γ-Al_2O_3 upon CO exposure. They concluded that CO adsorption leads to a disruption of small Rh clusters, resulting in formation of $Rh(CO)_2$. From XPS and ESR measurements they also observed that the oxidation state of Rh atoms changes to 1+ following CO admission. The disruption of Rh clusters and the formation of $Rh(CO)_2$ were confirmed by Solmosi et al.[7,8] and by Basu et al.[9,10] from IR studies.

In our previous papers,[11,12] it was shown by EXAFS spectroscopy that the morphology change of metal clusters by CO adsorption is not limited to Rh but takes place also for Ru. CO adsorption on small Ru clusters supported on γ-Al_2O_3 led to a disruption of Ru–Ru bonds and a formation of Al–O–$Ru(CO)_n$ species. Solymosi et al.[13] also observed from IR study that the CO-induced oxidative disruption of small Ru clusters supported on Al_2O_3 takes place. They proposed that the disruption is related to the reactivity of OH groups on the surface of Al_2O_3. Similar schemes have been proposed for Rh supported on Al_2O_3.[6-10]

The purpose of the present work is 2-fold. The first is to study the effect of the support on CO adsorption-induced morphology change in Ru metal particles. γ-Al_2O_3-, SiO_2-, MgO-, and TiO_2-supported Ru catalysts were prepared and characterized by the use of EXAFS before and after CO exposure. The second is to study whether the proposed scheme for disruption is correct or not. IR measuremenst on adsorbed CO and surface deuteroxyl groups were carried out to examine the role of hydroxyl group on the reaction.

† Institute for Molecular Science.
‡ Toyohashi University of Technology.

It was found that the structural change caused by CO adsorption takes place on γ-Al_2O_3 and MgO supports, but not on SiO_2 and TiO_2. IR absorption due to surface OD vanishes after CO adsorption on Ru/γ-Al_2O_3 and Ru/MgO but recovers after the desorption of CO. On the basis of the results obtained, a new scheme for the CO adsorption-induced disruption is presented.

Experimental Section

The 2 wt % supported Ru catalysts were prepared from $Ru_3(CO)_{12}$. γ-Al_2O_3, SiO_2, and TiO_2 were commercial materials having stated specific surface areas of 150, 300, and 150 m^2/g, respectively. These oxides were heated at 773 K, first in air for 10 h and then under vacuum for 2 h. MgO was prepared by heating $Mg(OH)_2$ under vacuum at 773 K. The specific surface area of the MgO powder obtained is 220 m^2/g from a BET adsorption measurement. The catalyst preparation was carried out with the same method as that in the previous work.[12] In short, $Ru_3(CO)_{12}$ was adsorbed from hexane solution in a flow of nitrogen at room temperature onto the support. The solvent was subsequently removed under a reduced pressure at room temperature. The sample was pressed into thin, self-supporting disks and placed in an in situ EXAFS or IR cell. The decomposition of $Ru_3(CO)_{12}$ on each support was carried out under vacuum at 723 K for 2 h. Then the catalyst was reduced with hydrogen at 723 K for 2 h and subsequently evacuated at the same temperature for 1 h.

The EXAFS measurements were performed with a new double-crystal X-ray spectrometer. The principle of the optics is the same as the one used for the previous studies,[12,14] except for modifications as follows: First, the power of the X-ray generator was upgraded from 12 kW to 18

(1) Rice, C. A.; Worley, S. D.; Curtis, C. W.; Guin, J. A.; Tarrer, A. R. *J. Chem. Phys.* **1981**, *74*, 6487.
(2) Worley, S. D.; Rice, C. A.; Mattson, G. A.; Curtis, C. W.; Guin, J. A.; Tarrer, A. R. *J. Phys. Chem.* **1982**, *86*, 2714.
(3) Worley, S. D.; Rice, C. A.; Mattson, G. A.; Curtis, C. W.; Guin, J. A.; Tarrer, A. R. *J. Chem. Phys.* **1982**, *76*, 20.
(4) van't Blik, H. F. J.; van Zon, J. B. A. D.; Huizinga, T.; Vis, J. C.; Koningsberger, D. C.; Prins, R. *J. Phys. Chem.* **1983**, *87*, 2264.
(5) van't Blik, H. F. J.; van Zon, J. B. A. D.; Koningsberger, D. C.; Prins, R. *J. Mol. Catal.* **1984**, *25*, 379.
(6) van't Blik, H. F. J.; van Zon, J. B. A. D.; Huizinga, T.; Vis, J. C.; Koningsberger, D. C.; Prins, R. *J. Am. Chem. Soc.* **1985**, *107*, 3139.
(7) Solymosi, F.; Pasztor, M. *J. Phys. Chem.* **1985**, *89*, 4789.
(8) Solymosi, F.; Pasztor, M. *J. Phys. Chem.* **1986**, *90*, 5312.
(9) Basu, P.; Panayotov, D.; Yates, J. T., Jr. *J. Phys. Chem.* **1987**, *91*, 3133.
(10) Basu, P.; Panayotov, D.; Yates, J. T., Jr. *J. Am. Chem. Soc.* **1988**, *110*, 2074.
(11) Mizushima, T.; Tohji, K.; Udagawa, Y. *J. Am. Chem. Soc.* **1988**, *110*, 4459.
(12) Mizushima, T.; Tohji, K.; Udagawa, Y. *J. Phys. Chem.* **1990**, *94*, 4980.
(13) Solymosi, F.; Rasko, J. *J. Catal.* **1989**, *115*, 107.
(14) Tohji, K.; Udagawa, Y.; Kawasaki, T.; Mieno, A. *Rev. Sci. Instrum.* **1988**, *59*, 1127.

0002-7863/90/1512-7887$02.50/0

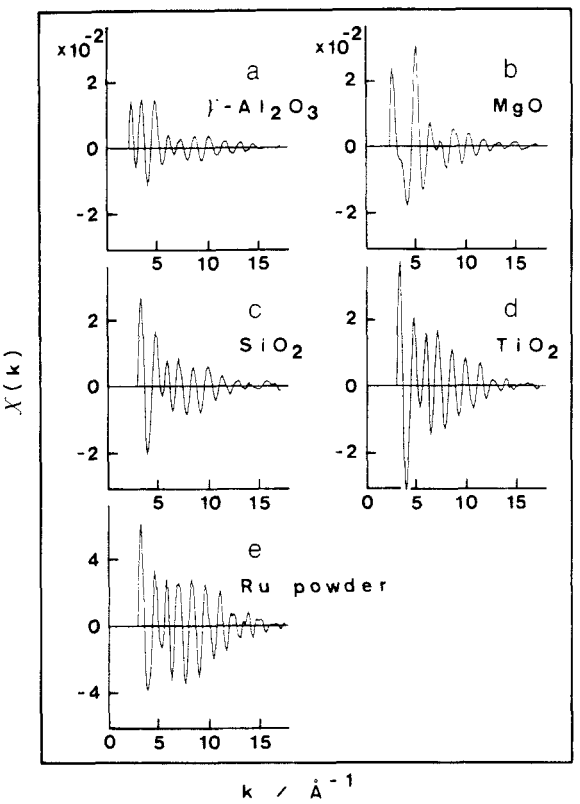

Figure 1. Extracted Ru K EXAFS oscillations $\chi(k)$ of (a) $Ru/\gamma\text{-}Al_2O_3$, (b) Ru/MgO, (c) Ru/SiO_2, and (d) Ru/TiO_2 after reduction and (e) Ru powder. Notice that the scale of the ordinate is different for part e.

kW. Second, a LiF(200) bent crystal which has higher reflectivity was used on the second monochrometer in place of the LiF(220) crystal employed in the previous work,[10] providing more photon flux. In this work Ge(660) and LiF(200) bent crystals were employed and the X-ray source was operated at 60 kV and 300 mA with a tungsten target. The resolving power of the spectrometer with a slit width of 100 μm is 9 eV at 17.5 keV as expressed as fwhm of Mo $K\alpha_1$ radiation. In addition to the improved resolving power compared with that in the previous work, the intensity of the incident X-ray beam is stronger by 1.5 times. Photon numbers exceeding 10^7 were accumulated at each data point. The EXAFS spectra were obtained at room temperature in an in-situ cell. For CO adsorption measurement, 200 Torr of CO was admitted. Analyses of EXAFS data were carried out as described in the previous paper.[12]

For IR measurements, 200 Torr of CO was admitted after the pretreatments described previously, kept in contact with the catalyst for about an hour, and then evacuated. IR spectra were subsequently recorded at room temperature by a Nicolet 7000 FT-IR spectrometer with a resolution of 2 cm^{-1}. The stretching vibration of OD was observed for the study of surface hydroxyl group, to avoid overlapping absorption of water in air. To replace surface OH with OD, D_2 was used instead of H_2 for reduction.

Results

EXAFS of Reduced Catalysts. Figures 1a–d and 2a–d show extracted EXAFS oscillations $\chi(k)$ and the associated k^3-weighted Fourier transforms for the Ru catalysts reduced and evacuated at 723 K. Here k represents momentum of photoelectrons. For comparison those of bulk Ru metal are also shown in Figures 1e and 2e. Significant differences are observed in EXAFS of each catalyst, indicating that the local structure around Ru depends on the support employed. A long oscillation toward high k values is a common feature in all of the spectra and is characteristic of heavy backscatterers like Ru as observed in bulk Ru shown in Figure 1e. Since Ru is the only heavy element in the samples, the neighboring atoms around Ru are also Ru, that is, the Ru atoms are in metal clusters. Compared with the bulk Ru, however, the amplitude of EXAFS oscillation of each catalyst varies with the support but is always smaller. The peak intensities in the associated Fourier transforms of the catalysts are consequently a factor of 2–8 times weaker than that of bulk Ru. Hence the Ru clusters are highly dispersed in every catalyst studied and the size of the Ru metal particles depends markedly on the support.

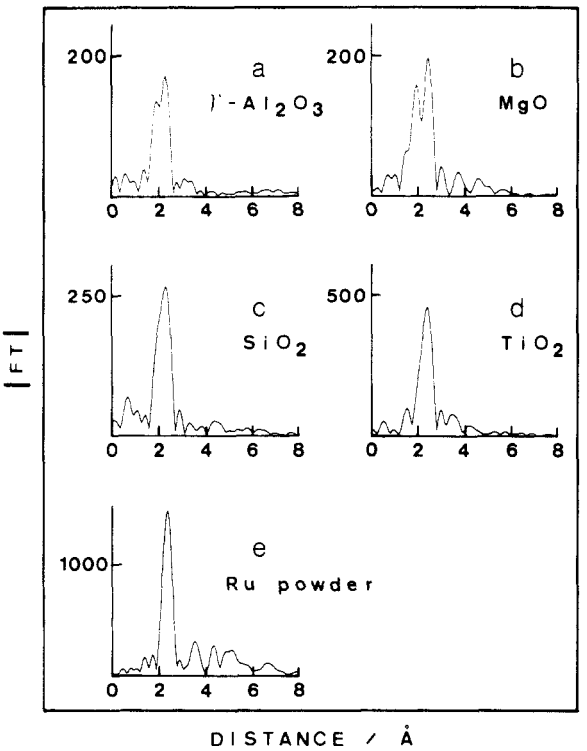

Figure 2. Fourier transforms of k^3-weighted EXAFS data of (a) $Ru/\gamma\text{-}Al_2O_3$, (b) Ru/MgO, (c) Ru/SiO_2, and (d) Ru/TiO_2 after reduction and (e) Ru powder.

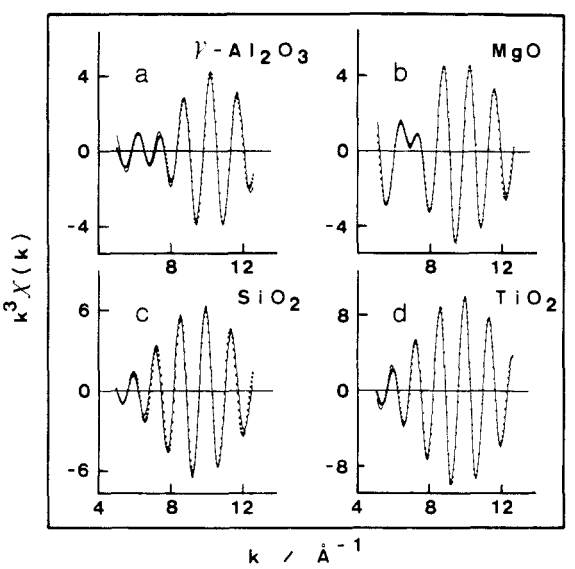

Figure 3. $k^3\chi(k)$ obtained by inverse Fourier transforms of main peaks (line) and those by curve-fitting calculations (dots) of (a) $Ru/\gamma\text{-}Al_2O_3$, (b) Ru/MgO, (c) Ru/SiO_2, and (d) Ru/TiO_2 after reduction. The two-shell model for $Ru/\gamma\text{-}Al_2O_3$ and Ru/MgO and the one-shell model for Ru/SiO_2 and Ru/TiO_2 are required to bring observation and calculation into agreement.

In addition to the peak height, there is a difference in the Fourier transforms of $Ru/\gamma\text{-}Al_2O_3$ and Ru/MgO from those of other catalysts studied here and from bulk Ru; a distinct peak is observed at a shorter distance than the main peak. As described in the previous paper,[12] this peak is attributed to support oxygen atoms bonded to Ru. The main peak in the Fourier transform of Ru/SiO_2 is asymmetric and is slightly broadened toward shorter distance, indicating that the Ru–O bond may also exist in Ru/SiO_2, but that of Ru/TiO_2 is almost symmetric.

To confirm the nature of the main peak in the Fourier transforms and to obtain detailed structural parameters, curve-fitting analyses[12] were attempted by assuming that Ru atoms in the

Table I. Structural Parameters of Ru Catalysts after Reduction[a]

	Ru–Ru			Ru–O		
	R, Å	*N*	σ, Å	*R*, Å	*N*	σ, Å
γ-Al_2O_3	2.58	2.5	0.09	2.09	0.8	0.00
MgO	2.61	2.6	0.07	2.09	3.4	0.09
SiO_2	2.64	4.0	0.08			
TiO_2	2.66	7.2	0.08			
Ru powder	2.68	(12.0)	0.06			
accuracy[b]	±0.02	±25[c]	±0.01	±0.03	±30[c]	±0.02

[a] *R*, interatomic distance; *N*, coordination number; σ, Debye–Waller factor. *N* of Ru powder is fixed to be 12. Experimentally derived parameters from Ru metal and RuO_2 were used for the calculations. [b] Estimated from variations in calculations with various sets of parameters for several measurements. [c] Percent.

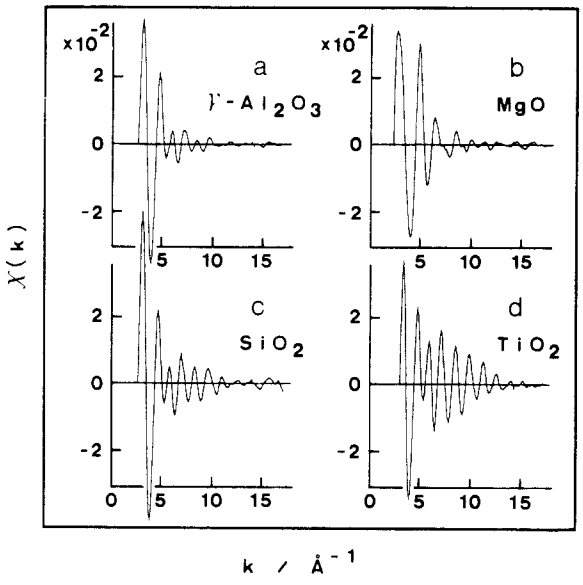

Figure 4. Extracted Ru K EXAFS oscillations χ(*k*) of (a) Ru/γ-Al_2O_3, (b) Ru/MgO, (c) Ru/SiO_2, and (d) Ru/TiO_2 after CO admission.

catalysts have either only one or two kinds of nearest neighbor shells: only ruthenium or both oxygen and ruthenium. Those results are shown in Figure 3. The one-shell model resulted in a satisfactory fit for Ru/SiO_2 and Ru/TiO_2 but failed to give a good fit for Ru/γ-Al_2O_3 and Ru/MgO, where the two-shell model is required to bring observation and calculation into agreement. This shows that the proportion of Ru atoms interacting with support oxygen is significant for Ru/γ-Al_2O_3 and Ru/MgO. Structural parameters thus obtained are summarized in Table I. The Ru–Ru average coordination numbers in the supported Ru metal clusters vary with support, but they are always much smaller than the bulk value of 12. The Ru–Ru interatomic distances in the catalysts are shorter than that of bulk Ru and different from each other, and it is worth noting that the Ru–Ru interatomic distance decreases with the decrease of the average coordination number. Contraction of the metal–metal interatomic distance is a feature that is often observed in small metal clusters.[15-18]

The Ru–O interatomic distance is 2.09 Å in both Ru/γ-Al_2O_3 and Ru/MgO, which is longer than the Ru–O distance of 1.97 Å in RuO_2. The average Ru–O coordination number of 3.4 in Ru/MgO is much larger than that in Ru/γ-Al_2O_3, 0.8. The larger oxygen coordination number in Ru/MgO is evidenced in Figure 1b from the amplitude in the low *k* region, where the scattering amplitude of low Z elements like oxygen is most evident.

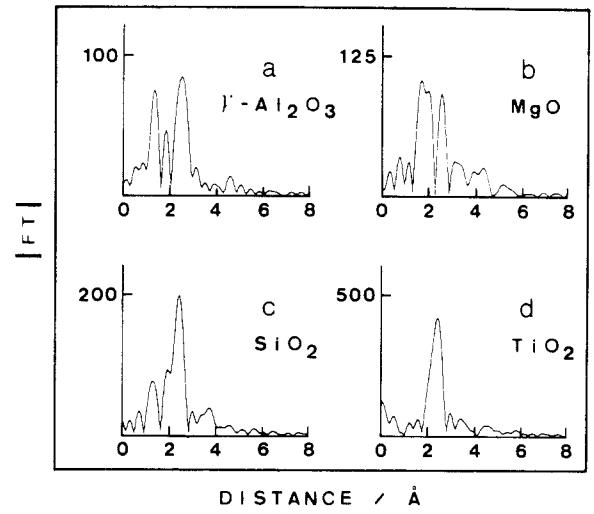

Figure 5. Fourier transforms of k^3-weighted EXAFS data of (a) Ru/γ-Al_2O_3, (b) Ru/MgO, (c) Ru/SiO_2, and (d) Ru/TiO_2 after CO admission.

EXAFS of the Catalysts after CO Admission. In Figures 4 and 5 extracted EXAFS oscillations and the associated k^3-weighted Fourier transforms of the catalysts after CO admission are shown. The effect of CO adsorption on EXAFS varies, depending on the support used. As is evident from a comparison between Figures 4a and 1a, CO adsorption on 2 wt % Ru/γ-Al_2O_3 leads to a drastic change of the local structure around Ru. The long oscillation characteristic of the heavy Ru backscatterers vanishes after CO admission, indicating that Ru–Ru bonds were disrupted. Three peaks are observed at about 1.37, 1.84, and 2.50 Å in the associated Fourier transform (without phase correction) shown in Figure 5a. As described in the previous paper[12] these are assigned to Ru–C, Ru–O(support), and Ru–(C)–O(oxygen of CO), respectively, suggesting that CO admission induces the disruption of small Ru metal clusters and formation of a new species of the form O-(support)–Ru–$(CO)_n$. The peak due to Ru–O(support) becomes conspicuous after the admission of CO, because it is now free from the overlapping peak due to Ru–Ru.

After the catalyst is heated under vacuum at 673 K for 30 min to desorb CO, the EXAFS spectrum becomes identical with that taken before CO exposure. This indicates that the Ru metal clusters are regenerated, that is, the structural change is reversible in adsorption/desorption cycles of CO.

EXAFS results in Figures 4b and 5b show that the CO adsorption-induced morphology change in Ru clusters also takes place on MgO support. As for Ru/γ-Al_2O_3, the amplitude of the oscillation at higher *k* becomes weak and damps rapidly with increasing *k* value, suggesting disruption of Ru–Ru bonds. Three peaks are observed in the associated Fourier transform, but the positions and the intensities are different from those for Ru/γ-Al_2O_3, indicating a difference in the form of CO species adsorbed on Ru. The small metal clusters are regenerated by evacuation at 673 K as is observed for Ru/γ-Al_2O_3.

In the case of Ru/SiO_2 the long EXAFS oscillation due to Ru backscatterers is nearly unchanged after CO admission as shown in Figure 3c, indicating that disruption of Ru metal clusters does not take place. The main peak in the associated Fourier transform shifts slightly toward longer distance. The expansion of the Ru–Ru bond may be caused by weakening with CO adsorption. In addition, a new peak which is assigned to Ru–C appears at shorter bond length than the main peak, suggesting that CO molecules adsorb on the surface of the small Ru metal particles. The interatomic distance of Ru–C is determined to be 1.86 Å from curve-fitting analysis, which is the same as that for Ru/γ-Al_2O_3. The EXAFS contributions of the coordination of Ru–Ru and Ru–(C)–O must both be embodied in the main peak. The Ru–O(support) bond may also be included in it.

On the other hand, almost no change is observed in EXAFS of Ru/TiO_2 after CO admission. The Ru–Ru interatomic distance

(15) Balerna, A.; Bernieri, E.; Picozzi, P.; Reale, A.; Santucci, S.; Burattini, E.; Mobilio, S. *Phys. Rev. B* **1985**, *31*, 5058.
(16) Montano, P. A.; Schulze, W.; Tesche, B.; Shenoy, G. K.; Morrison, T. I. *Phys. Rev. B* **1984**, *30*, 672.
(17) Moraweck, B.; Renouprez, A. J. *Surf. Sci.* **1981**, *106*, 35.
(18) Apai, G.; Hamilton, J. F.; Stohr, J.; Thompson, A. *Phys. Rev. Lett.* **1979**, *43*, 165.

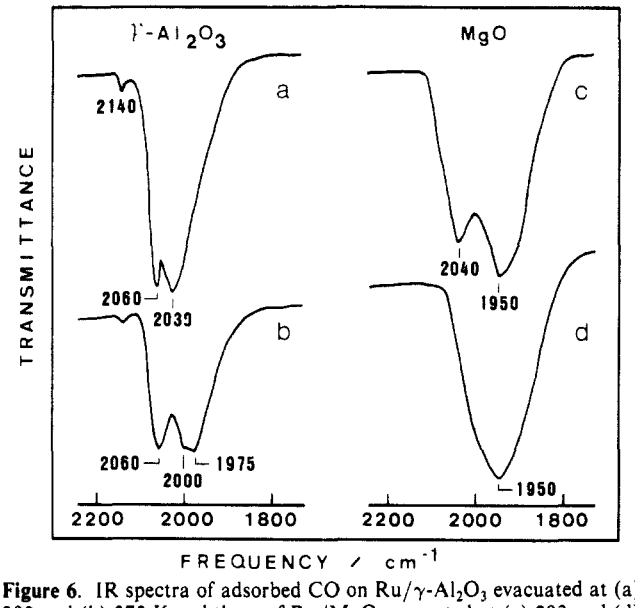

Figure 6. IR spectra of adsorbed CO on $Ru/\gamma\text{-}Al_2O_3$ evacuated at (a) 293 and (b) 373 K and those of Ru/MgO evacuated at (c) 293 and (d) 373 K after CO admission.

and average coordination number remain almost the same as those before CO admission. A peak due to Ru–C was not detected by EXAFS.

IR Spectra and a Comparison with EXAFS Results. In order to study the type of species formed by CO admission, IR measurements of adsorbed CO were attempted for $Ru/\gamma\text{-}Al_2O_3$ and Ru/MgO, in which the Ru–Ru bonds are disrupted by CO admission. These results are shown in spectra a and c of Figure 6. There are significant differences in the frequencies of the absorption bands in both spectra, indicating that the CO molecules are adsorbed on Ru in different manners. In the IR spectrum of $Ru/\gamma\text{-}Al_2O_3$ shown in Figure 6a there are two overlapping bands at 2060 and 2030 cm^{-1} with a shoulder at around 2000 cm^{-1}. A weak band is also observed at 2140 cm^{-1}. By evacuating at 373 K the band at 2030 cm^{-1} disappears and absorption bands remain at 2060 and 2000 cm^{-1} as is shown in Figure 6b. These bands behave similarly with increasing temperature, thus showing that these two belong to the same species. A new band is also observed at 1975 cm^{-1}.

For Ru/MgO two broad bands are observed at 2040 and 1950 cm^{-1} (Figure 6c). The higher frequency band disappeared after evacuation at 373 K, while the broad band with a maximum at around 1950 cm^{-1} remained as shown in Figure 6d. Hence there are two kinds of CO species at room temperature, but in evacuation at 373 K one of them is desorbed or transformed to the other form. Integrated absorption intensity does not change much, suggesting that transformation rather than desorption is dominant. Whichever is the case, only one kind of adsorbed CO remains on Ru after evacuation at the temperature. Its vibrational frequency indicates that this remaining CO on Ru/MgO is adsorbed in a different fashion from the CO on $Ru/\gamma\text{-}Al_2O_3$.

The EXAFS result, which is shown in Figure 7, is in accordance with the IR observation. The integrated area of the first two peaks in the Fourier transform, which correspond to Ru–C(of adsorbed CO) and Ru–O(of MgO), remains almost the same. The relative intensity has, however, changed after an evacuation at 373 K, indicating a change in the form of adsorbed CO.

IR measuremens were also carried out in OD stretching regions for $Ru/\gamma\text{-}Al_2O_3$ and Ru/MgO reduced with deuterium. Sharp bands at 2750 cm^{-1} in Figure 8a and at 2760 cm^{-1} in Figure 8d are attributed to isolated deuteroxyl groups on the surfaces of the support oxides.[19] After CO admission and evacuation at room temperature these bands diminish as shown in Figure 8, b and e, suggesting that the number of isolated OD groups are decreased by CO adsorption. In addition, a broad band appears at

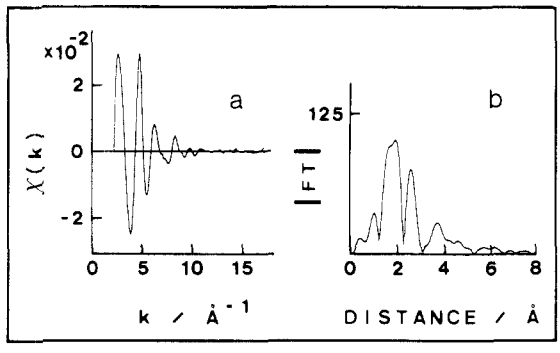

Figure 7. (a) Extracted EXAFS oscillation $\chi(k)$ and (b) the associated k^3-weighted Fourier transform of Ru/MgO evacuated at 373 K for 30 min after CO admission.

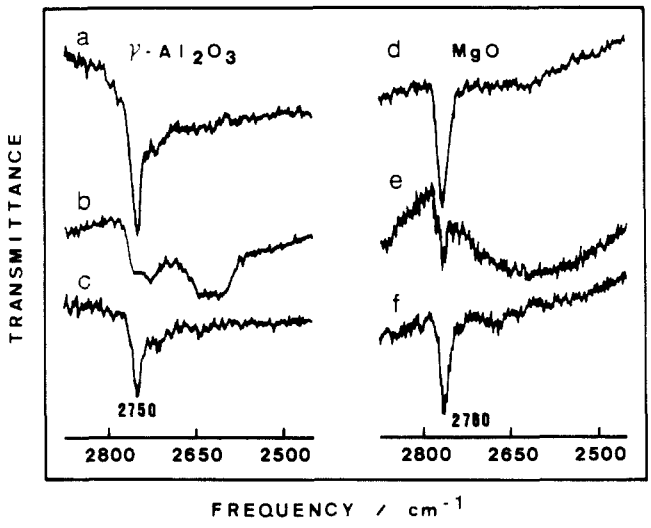

Figure 8. IR spectra in the ν_{OD} region of (a–c) $Ru/\gamma\text{-}Al_2O_3$ and (d–f) Ru/MgO: (a, d) after reduction with deuterium at 723 K; (b, e) after CO admission and evacuation at room temperature; (c, f) after evacuation at 673 K.

2670–2580 cm^{-1} for $Ru/\gamma\text{-}Al_2O_3$, where hydrogen-bonded deuteroxyl groups have an absorption band. A similar absorption band, although much weaker, is also observed at 2700–2500 cm^{-1} for Ru/MgO. The original spectra as shown in Figure 8, a and d, are recovered by evacuating the samples at 673 K as shown in Figure 8, c and f. This is in accordance with the EXAFS results that the structural changes are reversible with CO adsorption/desorption cycles.

Discussion

The Structure of Ruthenium after Reduction. The EXAFS results show that the environment around Ru atoms in the reduced catalyst depends significantly on the support. The low Ru–Ru coordination number indicates that the Ru metal particles are very small, making the detection of the bond between Ru and support oxygen possible. For $Ru/\gamma\text{-}Al_2O_3$ and Ru/MgO there are significant contributions from coordinated oxygen atoms to the EXAFS oscillation. The Ru–O distances are the same in both catalysts, but there is a large difference in the coordination numbers, suggesting that Ru particles are anchored on the supports through Ru–O bonds in different manners.

In our EXAFS results the average Ru–Ru coordination numbers are 2.5 in $Ru/\gamma\text{-}Al_2O_3$ and 2.6 in Ru/MgO, which are much smaller than the bulk value of 12, suggesting that the Ru atoms are in very small metal clusters. Greegor and Lytle[20] proposed a relationship between the metal cluster size and the average coordination number, assuming that the cluster has either sphere, cube, or monolayer disk. In this case, however, the cluster size cannot be determined for sure by the following reasons. First, the absolute value of N crucially depends on the mean free path

(19) Peri, J. B.; Hannan, R. B. *J. Phys. Chem.* **1960**, *64*, 1526.

(20) Greegor, R. B.; Lytle, F. W. *J. Catal.* **1980**, *63*, 476.

of the photoelectron, λ, in the solid. It is not sure that λ in such small clusters is the same as that of bulk metal, which is an assumption used in the calculation leading to Table I. Second, the cluster size is too small to define whether it is sphere, cube, or monolayer disk. The relative magnitude of the ratio of the coordination number for Ru and O should be, however, meaningful and can be a basis to understand the difference in metal–support interaction of the two supports. From Table I the Ru/O ratio is about 3 in $Ru/\gamma\text{-}Al_2O_3$ and about 0.8 in Ru/MgO; the number of oxygen atoms interacting with each Ru is from three to four times more on MgO than on $\gamma\text{-}Al_2O_3$. Thus it is plausible that each Ru atom is in atop sites on oxygen atoms of $\gamma\text{-}Al_2O_3$, while it is in a 3- or 4-fold hollow site on MgO. This model for Ru/MgO does not, however, agree with the crystal structure of MgO. The distance between the 3-fold hollow sites of the oxygen layer of MgO(111) plane and between the 4-fold hollow sites in MgO(100) is 2.98 Å in both, being fairly different from the observed Ru–Ru distance, 2.61 Å.

On the other hand, the model for $Ru/\gamma\text{-}Al_2O_3$ is consistent with chemisorption study. As reported in the previous paper,[12] hydrogen chemisorption occurs with a hydrogen atom to Ru ratio of 1.0 in 2 wt % $Ru/\gamma\text{-}Al_2O_3$, which implies that all Ru atoms are exposed to surface. The value in 4 wt % $Ru/\gamma\text{-}Al_2O_3$ decreases to 0.8; not all Ru atoms are on the surface. Thus, at lower concentration Ru atoms tend to form two-dimensional clusters, possibly each Ru atom being on top of oxygen atoms. At higher concentrations clusters start to grow three dimensionally, giving higher Ru–Ru coordination number and lower Ru–O coordination number.

For Ru/SiO_2 and Ru/TiO_2 a well-defined peak attributable to Ru–O is not observed in the Fourier transforms. The Ru–Ru coordination numbers are large relative to those of $Ru/\gamma\text{-}Al_2O_3$ and Ru/MgO. These indicate that the Ru particles are three dimensional.

Structure of $Ru/\gamma\text{-}Al_2O_3$ after CO Admission. The EXAFS study reported here clearly shows that the influence of CO exposure on the structure of Ru catalysts varies considerably with support. Disruption of Ru–Ru bonds takes place in ultradispersed $Ru/\gamma\text{-}Al_2O_3$. Three peaks in the Fourier transform, which are attributed to Ru–C, Ru–O(support), and Ru–(C)–O, suggest that CO molecules are adsorbed on Ru atoms anchored to support oxygen. From curve-fitting analysis with theoretical scattering parameters,[21] the distances of Ru–C and Ru–(C)–O are determined to be 1.86 and 3.10 Å, respectively. The former value is very close to the average Ru–C distance in $Ru_3(CO)_{12}$ (1.91 Å), thus the C–O interatomic distance is calculated to be 1.24 Å, which is a little longer than the average C–O distance in the carbonyl compound (1.14 Å). These support the assumption that the two peaks are associated with C and O atoms of CO molecules adsorbed on Ru.

IR spectroscopy demonstrates that there are several kinds of CO species adsorbed on Ru atoms.[13,22-24] As described in our previous paper,[12] the band at 2030 cm^{-1} is attributed to linearly adsorbed CO and the bands at 2060 and 2000 cm^{-1}, which become more prominent after evacuation at 373 K, are assigned to antisymmetric and symmetric stretching vibrations of twin type CO. The band at 1975 cm^{-1} is attributed to CO species bridged to two Ru atoms. This species is observed only after evacuation at 373 K with a regeneration of Ru clusters.[12] A weak band at 2140 cm^{-1} suggests the existence of multiply adsorbed CO,[22,24] but their importance can be neglected. By combining the IR and EXAFS results it is concluded that new species like Al–O–Ru–CO and $Al–O–Ru–(CO)_2$ are formed on the surface of $\gamma\text{-}Al_2O_3$ after CO admission at room temperature. Accordingly the Ru–C and Ru–(C)–O distances obtained by curve-fitting analyses of EXAFS should be the concentration weighted average values of the two species. The structure model is summarized in Figure 9a.

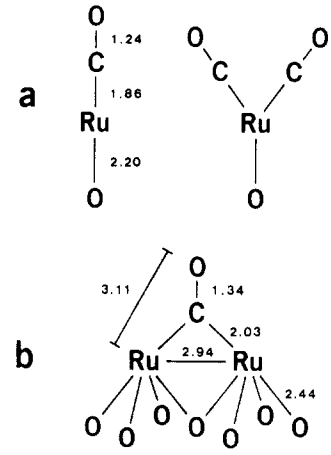

Figure 9. Geometries of $Ru–(CO)_n$ species formed on (a) $\gamma\text{-}Al_2O_3$ and (b) MgO after CO admission. The numerical values indicate interatomic distances in Å obtained by curve-fitting analyses. The interatomic distances shown in part a are the average values of the linear and twin type species.

Structure of Ru/MgO after CO Admission. The CO adsorption-induced dispersion of Ru particles is also observed in Ru/MgO, but the Fourier transform of Ru/MgO is different from that of $Ru/\gamma\text{-}Al_2O_3$. Marked differences in IR spectra for both the catalysts indicate that CO molecules are adsorbed on Ru atoms in a different manner. Guglielminotti[25] examined the CO adsorption on Ru/MgO by IR spectroscopy and observed two absorption bands at 2040 and 1950 cm^{-1} for high CO coverage, which is in good agreement with our results. According to him the higher and the lower frequency bands are assigned to linear and bridged CO species, respectively. Guglielminotti also found that the latter has higher thermal stability than the former, which is also confirmed from our IR measurement after evacuation at 373 K as is shown in Figure 6d.

Let us examine first the structure of Ru/MgO after an evacuation at 373 K, where only one CO species, the bridged CO, is expected from IR spectroscopy. In the bridged model, which is depicted in Figure 9b, the following conditions must be satisfied among the structural parameters derived from the analysis of EXAFS. First, the length of the Ru–C bond is expected to be longer for bridged CO than for linear CO as is observed in various carbonyl compounds.[26] Second, the difference between the Ru–C and Ru–(C)–O distances should be shorter than the interatomic distance of CO because the Ru–C–O angle is smaller than 180° in a bridged geometry. Third, Ru–Ru coordination should be detected. With these in mind the Fourier transforms in Figure 7b can be interpreted.

The broadness of the peak at a shorter distance indicates that it contains contributions from two coordination shells: carbon of bridged CO and support oxygen. The distances of Ru–C and Ru–O(support) are determined to be 2.03 and 2.44 Å, respectively, by a two-shell fitting analysis. The former is longer than Ru–C distances for the linear CO species observed in $Ru/\gamma\text{-}Al_2O_3$ and Ru/SiO_2 (1.86 Å in both) as expected.

In the bridge model, the peak at a longer distance also contains the contributions from two backscatterers: not only Ru but also the oxygen of CO. Indeed, although not shown here, the two-shell fit brought about far better agreement between the observation and calculation than one-shell fitting. The distances obtained by the two-shell fitting analysis are 3.11 Å for Ru–(C)–O and 2.94 Å for Ru–Ru. The latter is longer than that before CO exposure by as much as 0.3 Å, indicating the Ru atoms are no longer in metallic clusters after CO adsorption.

The difference between the interatomic distances of Ru–C and Ru–(C)–O is 1.08 Å, which is too short for the interatomic dis-

(21) Teo, B.; Lee, P. A. *J. Am. Chem. Soc.* **1979**, *101*, 2815.
(22) Kimura, T.; Okuhara, T.; Misono, M.; Yoneda, Y. *Nippon Kagaku Kaishi* **1982**, 162.
(23) Okuhara, T.; Kimura, T.; Kobayashi, K.; Misono, M.; Yoneda, Y. *Bull. Chem. Soc. Jpn.* **1984**, *57*, 938.
(24) Dalla Betta, R. A. *J. Phys. Chem.* **1975**, *79*, 2519.
(25) Guglielminotti, E. *Langmuir* **1986**, *2*, 812.
(26) Chini, P.; Longoni, G.; Albano, V. G. *Adv. Organomet. Chem.* **1976**, *14*, 285.

tance of CO, as expected for nonlinear bonding geometry. If a bridged CO species adsorbed on two Ru atoms has coordination distances of 2.03 Å for Ru–C, 3.11 Å for Ru–(C)–O, and 2.94 Å for Ru–Ru, then the interatomic distance of CO is calculated to be 1.34 Å, which is very close to that of bridged CO in $Fe_2(CO)_9$ (1.30 Å).[27] The Ru–Ru distance of 2.94 Å is close to the distances between the 3-fold hollow sites of the oxygen layer of MgO(111) plane or between the 4-fold hollow sites in MgO(100) (2.98 Å in both), suggesting that the Ru atoms exist in these sites. Taking account of the uncertainty of the coordination number, this picture is also consistent with the observed average coordination number of 3. The above results derived from EXAFS and IR spectroscopies confirm the existence of bridged CO species on MgO with the geometry shown in Figure 9b.

In addition to the bridged CO, a more weakly bound linearly adsorbed CO is expected to exist on Ru/MgO before evacuation at 373 K. Since the Ru–C distance for linear CO is expected to be different from that for bridged CO, the first peak in the Fourier transform must contain contributions from three kinds of coordination shells: carbon atoms of linear and bridged CO, and support oxygens. Since it is not reliable to make a three-shell fit, detailed analysis was not attempted. The change of the relative intensity in the first peak by evacuation at 373 K is, however, observed clearly from a comparison between Figures 5b and 7b, showing that the desorption of linear CO or the transformation to bridged CO takes place, the latter being favored from IR absorption intensity and EXAFS FT peak height.

Structure of Ru/SiO_2 and Ru/TiO_2 after CO Admission. The EXAFS results for Ru/SiO_2 and Ru/TiO_2 show that disruption of Ru–Ru bonds does not take place on these supports, and that the small Ru particles remain after CO exposure. CO adsorption on Ru was confirmed by IR spectroscopy for both catalysts, indicating that CO molecules are adsorbed on the surfaces of Ru clusters. In the Fourier transforms of EXAFS, a peak due to Ru–C was detected for Ru/SiO_2, but not for Ru/TiO_2. This is caused by the fact that the Ru particles supported on TiO_2 are large relative to those on the other support materials, and hence the ratio of the number of surface Ru atoms to total Ru atoms is too small to detect the influence of CO adsorption.

In summary, effects of CO adsorption on the morphology of Ru clusters are critically dependent on the support used; in $Ru/\gamma\text{-}Al_2O_3$, disruption of the metal clusters takes place and $Al\text{–}O\text{–}Ru(CO)_n$ (n = 1–2) are mainly formed; in Ru/MgO, Ru clusters also degrade but linear and bridged CO are formed, the latter being more stable; in Ru/SiO_2, although adsorption of CO was detected by EXAFS, disruption of the cluster cannot be observed; in Ru/TiO_2, almost no change was detected.

One of the reasons for the differences observed here must be in the metal cluster size in the catalysts studied. In the case of Ru/TiO_2 the coordination number of 7.2 is much larger than those of the other supports and accordingly the proportion of surface atoms is too small to observe any effect that occurs on the surface by EXAFS. Hence it cannot be ruled out that disruption takes place in the Ru/TiO_2 system if the Ru cluster size is small enough. Indeed Koningsberger et al.[28] noticed a partial disruption on Rh/TiO_2, where the Rh coordination number after reduction and before CO admission is 4.4.

Mechanism of the CO-Adsorption-Induced Oxidative Disruption. On the basis of an IR study of Ru/Al_2O_3, Solymosi et al.[13] observed a consumption of isolated OH group on Al_2O_3 with CO adsorption. They proposed that reactions between a transitory surface species $Ru(CO)_n$ and a surface OH group lead to oxidative disruption, as is typically expressed in eqs 1–3.

$$Ru_x + 2CO = Ru_{x-1}CO + Ru^0CO \quad (1)$$

$$Ru^0CO + CO = Ru^0(CO)_2 \quad (2)$$

$$Ru^0(CO)_2 + OH^- = Ru^+(CO)_2 + O^{2-} + \tfrac{1}{2}H_2(g) \quad (3)$$

(27) Powell, H. M.; Ewens, R. V. G. *J. Chem. Soc.* **1939**, 286.
(28) Koningsberger, D. C.; van't Blik, H. F. J.; van Zon, J. B. A. D.; Prins, R. *Proceedings of the International Congress on Catalysts*; Academic Press: New York, 1984; Vol. 123.

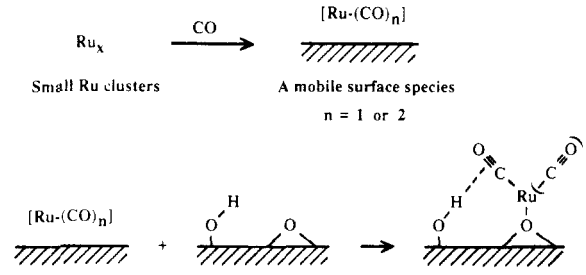

Figure 10. A proposed mechanism of the CO adsorption-induced oxidative disruption of small Ru clusters on $\gamma\text{-}Al_2O_3$. The broken line represents a hydrogen bond between CO adsorbed on Ru and the surface OH group.

Basu et al.[9,10] also observed the consumption of isolated OH groups as $Rh(CO)_2$ forms in $Rh/\gamma\text{-}Al_2O_3$ and Rh/SiO_2 by IR spectroscopy and proposed a similar reaction scheme, where mobile surface species Rh(CO) reacts with surface hydroxyl groups in the following way.

$$RhCO + OH = ORh^+CO + \tfrac{1}{2}H_2(g) \quad (4)$$

$$ORh^+CO + CO = ORh^+(CO)_2 \quad (5)$$

They also found the absorbance increases in the associated ν_{OH} region and related this band not to a simple conversion of isolated OH groups into associated ones but to a CO physisorption on OH groups via H bonding. van't Blik et al.[6] also proposed a reaction between rhodium carbonyl and surface OH as the most likely explanation of the oxidative disruption of Rh/Al_2O_3 by CO adsorption.

Since the intensity of OH absorption decreases with CO adsorption, surface hydroxides must be involved in the reaction. Doubt can be cast, however, about the validity of the mechanisms presented above. Although all these mechanisms require an evolution of $H_2(g)$, van't Blik et al. failed in an attempt to detect H_2 by gas chromatography. We also could not find any evidence for H_2 formation either by gas chromatographic or more sensitive mass spectroscopic detection.[12] These observations, however, still cannot rule out the possibility that the detection systems may have been just too insensitive to detect hydrogen gas generation.

Our IR spectroscopic observation shown in Figure 8 supports gas chromatographic and mass spectroscopic results. Solymosi et al. and Basu et al. observed that for surface OH on Ru/Al_2O_3 and on Rh/Al_2O_3, the absorption intensity of isolated hydroxyl groups decreases and that of associated (hydrogen bonded) hydroxyl groups increases. In this study we also observed a decrease of isolated OD group and a growth of the broad band in the associated ν_{OD} vibration region on $\gamma\text{-}Al_2O_3$ and MgO. On top of that, however, absorption intensity due to isolated ν_{OD}, though not fully, is recovered by evacuation at 673 K which causes CO desorption. The regeneration of OD with CO desorption is proof that deuterium remains on the catalyst after the disruption of the Ru cluster. Thus, although the evolution of H_2 cannot be completely ruled out, most of the OH consumption takes place not as hydrogen gas evolution but as a transformation to associated form. Basu et al. attributed the growth of broad bands to the associated surface OH on which CO is physisorbed. These bands, however, were not observed when CO was introduced to $\gamma\text{-}Al_2O_3$ or MgO without Ru. This suggests that the appearance of associated hydroxyl groups is somehow related to mobile surface species like $Ru(CO)_n$.

In summary, the following scheme, which is depicted in Figure 10, can be postulated as the most likely process after CO adsorption on Ru/Al_2O_3 or Rh/Al_2O_3. First, mobile surface species Ru(CO) or $Ru(CO)_2$ are liberated from Ru clusters by CO adsorption.

$$Ru^0{}_x + CO \rightarrow Ru(CO) \text{ or } Ru(CO)_2 \quad (6)$$

Then these mobile surface species migrate across the oxide surface and are trapped by isolated OH groups. The hydrogen atom of the OH group is not replaced with the $Ru(CO)_n$ as is proposed

in eq 4 but remains on the catalyst surface.

Basu et al. has stated that a linear correlation between the loss of OH intensity in the isolated OH and the gain in integrated intensity in the associated OH species does not *seem* to exist, which is not in perfect accordance with the scheme shown in Figure 10. Accordingly, further studies concerning the reaction mechanism are definitely required, because reactions of small metal clusters in supported catalysts with adsorbates may play a crucial role in heterogeneous catalysis.

Registry No. Ru, 7440-18-8; MgO, 1309-48-4; TiO_2, 13463-67-7; CO, 630-08-0.

Slow Dissociations of Thiophenol Molecular Ion. Study by TRPD and TPIMS

James D. Faulk,† Robert C. Dunbar,*,† and Chava Lifshitz*,‡

Contribution from the Chemistry Department, Case Western Reserve University, Cleveland, Ohio 44106, and Department of Physical Chemistry and The Fritz Haber Research Center for Molecular Dynamics, The Hebrew University of Jerusalem, Jerusalem 91904, Israel.
Received March 12, 1990

Abstract: Dissociation of thiophenol molecular ion to yield competitive product ions at m/z 84 ($C_4H_4S^+$) and 66 ($C_5H_6^+$) was studied by several techniques. Time-resolved photodissociation at 308 nm (4.20 eV ion internal energy) in the ICR ion trap gave rate constants of 1.3×10^5 s^{-1} for m/z 84 formation and 8×10^4 s^{-1} for m/z 66 formation, and at 355 nm (3.66 eV ion internal energy) it gave 2.8×10^3 s^{-1} for m/z 84 formation, with m/z 66 not observed at this wavelength. Time-resolved photoionization mass spectrometry at 800 μs trapping time gave thresholds of 2.9 eV for m/z 84 formation and 3.2 eV for m/z 66 formation; the photoionization efficiency curves cross at approximately 4 eV internal energy so that m/z 66 is more abundant at energies above this; at 20-μs trapping a kinetic shift of approximately 0.2 eV was observed relative to 800-μs trapping. MIKES spectra indicated a low average kinetic energy release for metastable ion decomposition, $\langle T \rangle = 52 \pm 5$ meV, for m/z 66, and a higher kinetic energy release, $\langle T \rangle = 151 \pm 5$ meV, for m/z 84. RRKM modeling of these dissociations was successful, using a very loose transition state ($\Delta S^{\ddagger}(1000\ K) = 14$ eu) and a critical energy of 3.2 eV for m/z 66 formation, a tighter transition state ($\Delta S^{\ddagger}(1000\ K) = 2.74$ eu) and a critical energy of 2.9 eV for m/z 84 formation. With use of TRPD as an ion-thermometric tool, collisional cooling of hot thiophenol ions by collisions with neutral thiophenol was observed and a collisional cooling rate constant of 4×10^{-10} $cm^3 \cdot molecule^{-1} \cdot s^{-1}$ was measured.

Introduction

Because charged molecules are easy to manipulate and detect, the study of unimolecular dissociation kinetics has received much impetus from ion dissociations studied in various kinds of mass spectrometers. The most clear-cut and satisfactory experiments of this kind have taken advantage of the ability of photons to deposit precisely known increments of energy, affording to various photoionization and photodissociation experiments the advantage of excellent knowledge of the internal energy of the fragmenting molecule.

Recent advances in studying dissociation kinetics by both photoionization and photodissociation have opened up ways of observing unimolecular dissociations with very low rates, having dissociation time constants of several milliseconds or longer. The time-resolved photoionization mass spectrometry (TPIMS) experiment in the quadrupole ion trap[1] and the time-resolved photodissociation (TRPD) experiment in the ion cyclotron resonance (ICR) ion trap[2] are two such techniques that are finding application to a variety of slow-dissociation systems.

The dissociation of thiophenol ion in the region of 3.5–4.5 eV internal energy is a slow dissociation about which little quantitative kinetic information has been available, and the application of these two techniques has provided the first rate values for this system. In the internal energy regime of interest here, the ion dissociates competitively to two products according to

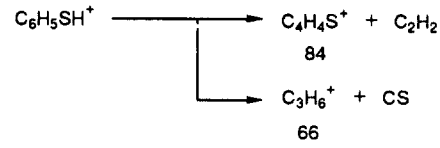

Initial TRPD observations[3] of the rate of m/z 66 production from thiophenol ion photodissociation at 308 nm indicated a unimolecular rate constant near 10^5 s^{-1}. This rate was strikingly faster than the approximately 1×10^3 s^{-1} predicted from reasonable RRKM modeling of the process. A tight transition state was assumed in this initial modeling of this system, considered to be almost surely involved in such a rearrangement fragmentation.

This unexpected result inspired a more extensive examination of the system, to investigate whether (a) the initial TRPD observations were flawed, (b) the thermochemically derived activation energy of 3.2 eV used in the modeling was too high, (c) the assumption of a tight transition state should be reconsidered, or (d) RRKM theory (which involves statistical or quasiequilibrium theory assumptions) is violated in this case. Experiments with the TRPD and TPIMS techniques, along with auxiliary work with Fourier-transform mass spectrometry, two-photon photodissociation, and MIKES, have been used to characterize the dissociation channels yielding both m/z 66 and 84, leading finally to a satisfactory picture of this system in the slow-dissociation regime.

Experimental Section

The ICR–TRPD experiments were carried out as has been described in detail in previous publications,[2] using the phase-sensitive-detection ICR

† Case Western Reserve University.
‡ Archie and Marjorie Sherman Professor of Chemistry. The Hebrew University of Jerusalem.

(1) (a) Lifshitz, C.; Goldenberg, M.; Malinovich, Y.; Peres, M. *Org. Mass Spectrum.* **1982**, *17*, 453. (b) Malinovich, Y.; Arakawa, R.; Haase, G.; Lifshitz, C. *J. Phys. Chem.* **1985**, *89*, 2253. (c) Ziesel, J. P.; Lifshitz, C. *Chem. Phys.* **1987**, *177*, 227. (d) Ohmichi, N.; Malinovich, Y.; Ziesel, J. P.; Lifshitz, C. *J. Phys. Chem.* **1989**, *93*, 2491. (e) Lifshitz, C.; Ohmichi, N. *J. Phys. Chem.* **1989**, *93*, 6329.

(2) (a) Dunbar, R. C. *J. Phys. Chem.* **1987**, *91*, 2801. (b) So, H. Y.; Dunbar R. C. *J. Am. Chem. Soc.* **1988**, *110*, 3080. (c) Dunbar, R. C. *J. Phys. Chem.* In press. (d) Dunbar, R. C. *J. Am. Chem. Soc.* **1989**, *111*, 5572.

(3) Faulk, J. D.; Dunbar, R. C. Proceedings of the 37th ASMS Conference on Mass Spectrometry and Allied Topics, Miami Beach, FL, May 21–26, 1989, p 254.

(4) Faulk, J. D.; Dunbar, R. C. *J. Phys. Chem.* In press.

(5) Asamoto, B.; Dunbar, R. C. *Chem. Phys. Lett.* **1987**, *139*, 225.

0002-7863/90/1512-7893$02.50/0